Angewandte Chemie
Eine Zeitschrift der Gesellschaft Deutscher Chemiker

Supporting Information

Magnetic Micromotors for Multiple Motile Sperm Cells Capture, Transport, and Enzymatic Release

Haifeng Xu, Mariana Medina-Sánchez, and Oliver G. Schmidt*

anie_202005657_sm_miscellaneous_information.pdf

Experimental Section

Microcarrier optimization. Arrays of microcarriers were fabricated by 3D laser lithography (Nanoscribe). Briefly, a dip-in negative-tone photoresist (IP-DIP, Nanoscribe) was drop-casted onto fused silica glass substrates. The prepared sample was then polymerized specifically at preprogrammed exposure positions by two-photon absorption (780 nm). The design of the microcarriers was programmed with Describe software (Nanoscribe). The samples were then dried in a critical point dryer (CPD, Autosamdri®-931, Tousimis) after 20 min of development in mr-Dev 600 (Micro Resist) and 3 min of washing in isopropanol. The dried samples were coated with 2 nm TiO_2 and 50 nm Fe by electron beam evaporation (Edwards auto 500 e-beam, Moorfield). The metal-coated samples were also immersed in Pluronic® F-127 solution for 1 h at 37 °C and rinsed with water and SP-TALP for subsequent experiments to avoid unspecific adhesion of target cells.

The flow simulation was performed in Solidworks, in which the rotation frequency of the microcarriers was set to 20 Hz in general and 40 Hz in the high frequency mode. Water at 25 °C was used as the model fluid. Only laminar flow was considered due to the micromotor movement in the conditions at low Reynolds number (Re << 0.1).[9] Simulation were based on the Navier-Stokes equation:[10,11]

$$\rho\left(\frac{\partial u}{\partial t}+\frac{\partial u}{\partial x}+\frac{\partial u}{\partial y}+\frac{\partial u}{\partial x}\right)=\frac{\partial P}{\partial x}+\mu\left(\frac{\partial^2 u}{\partial x^2}+\frac{\partial^2 u}{\partial y^2}+\frac{\partial^2 u}{\partial z^2}\right)+\rho g_x$$

Where $\rho, u, t, x, P \; and \; g_x$ represent the fluid density, fluid velocity, time, flow dimension$(x, y \; or \; z)$, internal pressure, and acceleration due to gravity at given dimension $(x, y \; or \; z)$, respectively.

Scanning electron microscopy (Zeiss Nvision 40, Carl Zeiss Microscopy GmbH) was performed to evaluate the microcarriers printing quality. Images were taken under a working voltage of 3 kV in the secondary electron imaging mode at a working distance of 5 mm.

Swimming performance of microcarriers. Microcarriers were dispersed in SP-TALP at a concentration of ~100 structures per mL. Microcarrier locomotion was realized by rotation of an orthogonal magnetic field (MFG 100, MagnebotiX). Immotile sperm carrying was performed by dispersing immotile sperms in SP-TALP at concentration of 10^6 sperms/mL. Microcarriers were also evaluated in saliva, 4× diluted bovine blood, mimicked oviduct fluid and the *ex vivo* oviduct channels, wherein the mimicked oviduct fluid was prepared at viscosity of 5.9 mPa·s. In short, methylcellulose was dispersed in SP-TALP at a concentration of 0.4%. The dispersion was stored at 4 ℃ for 24 h for swelling. After that, polystyrene microparticles of 10 μm diameter were dispersed in the prepared solution at a concentration of ~3×10^5 particles per mL to mimic the floating epithelial cells in the oviduct fluid. *Ex vivo* oviducts were taken from non-used sources from running projects of generating mutant and rederiving mouse lines by *in vitro* fertilization (IVF) with frozen sperm in the Transgenic Core Facility of the Max Planck Institute of Molecular Cell Biology and Genetics lead by Ronald Naumann according to established protocols. The Transgenic Core facility holds active permissions for the work with mouse embryos and works under the principles of the 3Rs with animals living under specific pathogen free (SPF) conditions. Two isolated mouse oviducts were cut open and fixed in a parafilm channel as the top and bottom walls to form a tissue tunnel. The height of the tissue tunnel was controlled to be ca. 0.26 mm by adjusting the parafilm thickness. After that, the whole channel was filled with mimicked oviduct fluid. All the experiments involving sperm in this study were performed at 37 ℃. An inverted microscope (Nikon) was used to monitor the locomotion. Recorded videos were further treated with ImageJ.

The structural stability of microcarriers was evaluated in SP-TALP. Briefly, microcarriers were dispersed in SP-TALP in a microchannel. Magnetic field of ca. 10 mT at 65 Hz was applied on the sample for 20 min. The microcarriers were then incubated at 37 °C with 95% humidity and 5% CO_2. After 3 days, the same magnetic field was applied to steer the microcarriers. 31 microcarriers were evaluated. Optical images were captured by an inverted microscope (Nikon). Recorded videos were further treated with ImageJ.

Microflake optimization. Microflakes were fabricated by using a micro-emulsion and milling method.[12] Briefly, BSA (Sigma-Aldrich) and HA (Sigma-Aldrich) were dissolved in SP-TALP at a concentration of 6% and 1.5%, respectively. The solution was mixed with sunflower oil, Span-80, Tween-80 and ethanol at ratio of 5:100:5:5:1. The emulsion system was stabilized for 1 h. Size of microflakes were regulated by varying the stirring speed and the emulsion composition. Then 1-ethyl-3-(3-dimethylaminopropyl)carbodiimide (EDC) (Sigma Aldrich) was slowly dropped in at a final concentration of 15 μg/mL to cross-link HA. After that, the system was heated at 75 °C for 0.5 h for obtaining the BSA/HA microbeads.[13] After washing, microbeads were dried and milled in a mortar at 4 °C to get the final microflakes with exposed HA microparticles. For SEM characterization, microbeads and microflakes were coated with 10 nm Au and attached on the stub with a carbon tape.

The prepared microflakes were directly used for sperm capturing. First, sperms were prepared using a swim-up method reported elsewhere.[14] After that, sperm capturing was accomplished by co-incubating the microflakes with purified sperm solution at concentration of 10^6 sperms/mL. Sperm capturing was monitored under an inverted microscope and the capturing number was calculated out of the recorded videos. DOX-HCl loaded sperms were prepared as reported in our previous work.[6]

Biocompatibility evaluation. HeLa cells were cultured as a model to evaluate the biocompatibility of the microcarrier and the microflake. Briefly, 20 wells from two 12-well

plates were filled with cell media with 2 mL in each and divided in 5 groups. Separately, 20 μL media, 20 μL SP-TALP, 20 μL microflake solution (2.5 mg/mL, SP-TALP), 20 μL microcarrier dispersion (20000 per mL, SP-TALP) and 20 μL microflake and microcarrier at the same density were introduced in each group. HeLa cells were seeded in all groups at a concentration of 2×10^5 /mL. Magnets were placed underneath the samples throughout the culture duration. After 72 h of incubation, cells were trypsinized off and redispersed in cell media. Trypan blue was used to stain cells directly before cell counting. Only live cells were counted. Cell viability was calculated as a ratio of live cell numbers in the specific group relative to the blank control with only HeLa media.

Sperm transport and enzymatic release. Frozen bovine sperms were purchased from Masterrind GmbH. Microfluidic chips as working platforms were fabricated using a molding method as reported in our previous work. Briefly, negative photoresist SU-8 (SÜSS Microtec) was spin-coated on a silicon wafer at a speed of 2000 r.p.m. After essential prebaking, the prepared sample was patterned by maskless lithography (μPG 501, Heidelberg Instruments). The molding master was then prepared after post and hard baking process. PDMS (Dow Corning) were molded on the master and heated at 65 ℃ for 3 h to gel. After that, cleaned glass substrates as well as the PDMS channel were treated by oxygen plasma. Then the PDMS channels were bonded to glass substrates through siloxane bonds and heated at 65 ℃ for 2 h. The narrowest part of the constriction channel was about 500 μm to mimic the oviduct structure. The microchip was firstly filled with SP-TALP. Then the microcarriers were introduced in the chamber together with the sperm-immobilized microflake which was picked up and purified in advance to avoid the disturbance of free sperm. After the transport finished, the microcarrier was moved backward by unscrewing it. To release the sperm, trypsin-EDTA was introduced through Inlet 2 at a final concentration of 100 μg/mL. Sperm release was recorded over time for the counting of release number.

The sperm motility was evaluated by using 3.5 cm dishes which were in advance immobilized with microflakes for sperm binding. Briefly, 0.5 mL of microflake dispersion at a concentration of 500 μg/mL was introduced in the 3.5 cm dish. The prepared dishes were then dried in nitrogen so that the microflakes were immobilized on the substrate of the dishes due to electrostatic force. Cryopreserved sperm were recovered rapidly at 37 °C for 2 min and washed twice in SP-TALP by centrifugation at 300 g. Sperm capturing was performed by adding 1.5 mL sperm solution at a concentration of 10^7 sperm/mL in the prepared dish. After 10 min incubation at 37 °C, the dishes were washed three times with SP-TALP to remove the free sperm and filled again with 1.5 mL SP-TALP. Sperm release was realized by adding trypsin-EDTA at a final concentration of 100 μg/mL. Free sperm without any capturing process were added with the same amount of trypsin for comparison. Untreated sperms served as blank control. The sperm motility was derived from the recorded videos with ImageJ.[15]

Evaluation for potential application as a drug delivery system. Doxorubicin hydrochloride (DOX-HCl) was used as a model drug and loaded in sperms as reported elsewhere.[6] HeLa spheroids were prepared as a tumor model as reported elsewhere.[6] Briefly, spheroids were obtained by seeding 2×10^4 HeLa cells in a microplate well with cell-repellent surface (Bio-greiner). After 3 days stabilization, all the spheroids were transferred to a PDMS microchamber in 0.3 mL serum free media with 50 μg/mL trypsin. MC3 microcarriers and sperm immobilized microflakes were obtained as mentioned before. The drug delivery experiment was performed by using a MC3 microcarrier to transport a microflake immobilized with DOX-HCl loaded sperms towards a HeLa spheroid. DOX-HCl distribution was observed by fluorescence microscopy (Cellobserver, Zeiss) at excitation of 485 nm. Fetal bovine serum (FBS) was introduced 20 min after the transport to terminate the trypsinization.

The anticancer effect experiment was performed by manually transporting 10 microflakes by a microcapillary pipette onto the above-mentioned HeLa spheroids in the PDMS

microchamber. Control samples were treated respectively with 10 bare microflakes, 10 microflakes immobilized with unloaded sperms and the same amount of cell media in the untreated spheroid as bare control. After 48 h of culture, the anticancer effect was evaluated by quantifying the reattachment rate as reported elsewhere.[16] In brief, the spheroids were disintegrated by trypsin and reseeded into 12-well plates. After 12 h of attachment, cells adhered on the plates were counted to calculate the reattachment rate.

References

[1] V. Magdanz, S. Sanchez, O. G. Schmidt, *Adv. Mater.* **2013**, *25*, 6581–6588.

[2] I. S. M. Khalil, V. Magdanz, S. Sanchez, O. G. Schmidt, S. Misra, *J. Micro-Bio Robot.* **2014**, *9*, 79–86.

[3] V. Magdanz, M. Medina-Sánchez, Y. Chen, M. Guix, O. G. Schmidt, *Adv. Funct. Mater.* **2015**, *25*, 2763–2770.

[4] M. Medina-Sánchez, L. Schwarz, A. K. Meyer, F. Hebenstreit, O. G. Schmidt, *Nano Lett.* **2016**, *16*, 555–561.

[5] V. Magdanz, M. Guix, F. Hebenstreit, O. G. Schmidt, *Adv. Mater.* **2016**, *28*, 4084–4089.

[6] H. Xu, M. Medina-Sanchez, V. Magdanz, L. Schwarz, F. Hebenstreit, O. G. Schmidt, *ACS Nano* **2018**, *12*, 327–337.

[7] C. Chen, X. Chang, P. Angsantikul, J. Li, B. Esteban-Fernández de Ávila, E. Karshalev, W. Liu, F. Mou, S. He, R. Castillo, Y. Liang, J. Guan, L. Zhang, J. Wang, *Adv. Biosyst.* **2018**, *2*, 1700160.

[8] I. S. M. Khalil, A. Adel, D. Mahdy, M. M. Micheal, M. Mansour, N. Hamdi, S. Misra, *APL Bioeng.* **2019**, *3*, 26104.

[9] S. J. Dhawan, R. Narasimha, *J. Fluid Mech.* **1958**, *3*, 418–436.

[10] R. G. Winkler, *Eur. Phys. J. Spec. Top.* **2016**, *225*, 2079–2097.

[11] P. M. Gresho, R. L. Sani, *Incompressible Flow and the Finite Element Method. Volume 2: Incompressible Flow and Finite Element*, John Wiley And Sons, Inc., New York, NY (United States), **1998**.

[12] Z. Zhou, Z. Yang, L. Kong, L. Liu, Q. Liu, Y. Zhao, W. Zeng, Q. Yi, D. Cao, *J. Macromol. Sci. Part B Phys.* **2012**, *51*, 2392–2400.

[13] I. Hayakawa, J. KAJIHARA, K. MORIKAWA, M. ODA, Y. FUJIO, *J. Food Sci.* **1992**, *57*, 288–292.

[14] A. Volpes, F. Sammartano, S. Rizzari, S. Gullo, A. Marino, A. Allegra, *J. Assist. Reprod. Genet.* **2016**, *33*, 765–770.

[15] J.-Y. Tinevez, N. Perry, J. Schindelin, G. M. Hoopes, G. D. Reynolds, E. Laplantine, S. Y. Bednarek, S. L. Shorte, K. W. Eliceiri, *Methods* **2017**, *115*, 80–90.

[16] H. Xu, M. Medina-sánchez, D. R. Brison, R. J. Edmondson, S. S. Taylor, L. Nelson, K. Zeng, S. Bagley, C. Ribeiro, P. R. Lina, E. Lucena, C. K. Schmidt, O. G. Schmidt, *arXiv:1904.12684* **2019**.

Supporting Information Figures

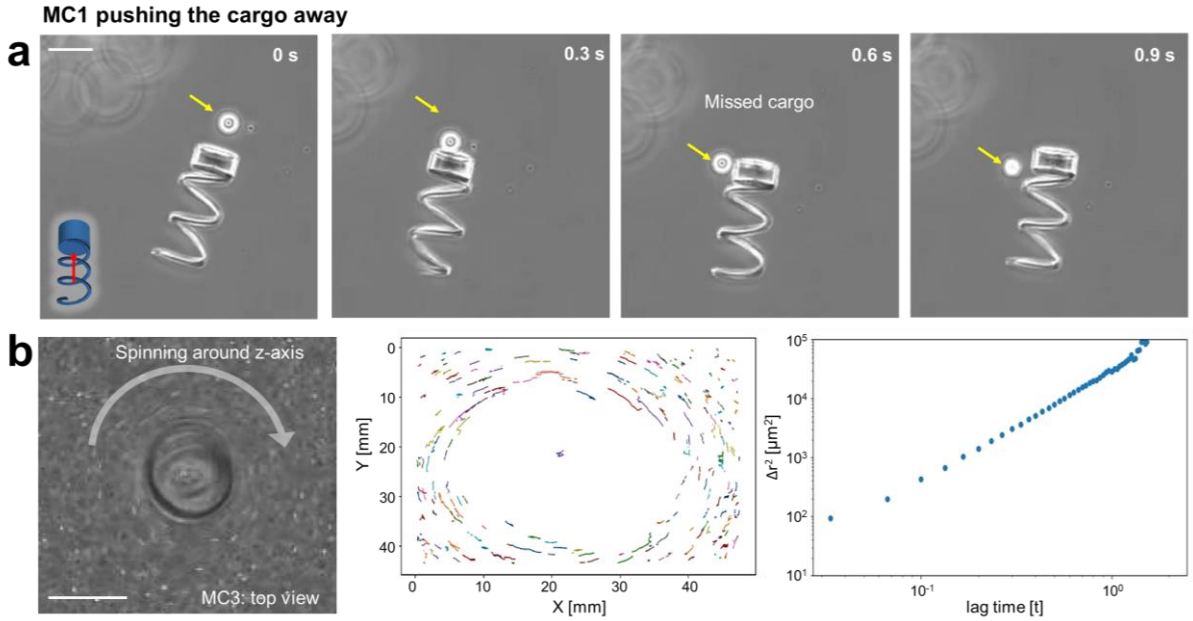

Figure S1. Cargo capturing and transport by the microcarrier based on the hydrodynamic vortex. (a) MC1 microcarrier swimming towards a 40 μm polystyrene particle (model cargo). Scale bar: 50 μm. (b) Fluid flow field around MC3 when rotating around the z-axis, showing the circular trajectories by the tracer particles in its vicinity. Particles in the close vicinity were not tracked due to the high density of particles which created artifacts during particle automatic tracking. On the right side, the ensemble mean square displacement (MSD) for all tracer particles in the presence of the rotating MC3 carrier is shown. Particle size: 5 μm in diameter. Magnetic field: 65 Hz at 10 mT. Scale bar: 50 μm.

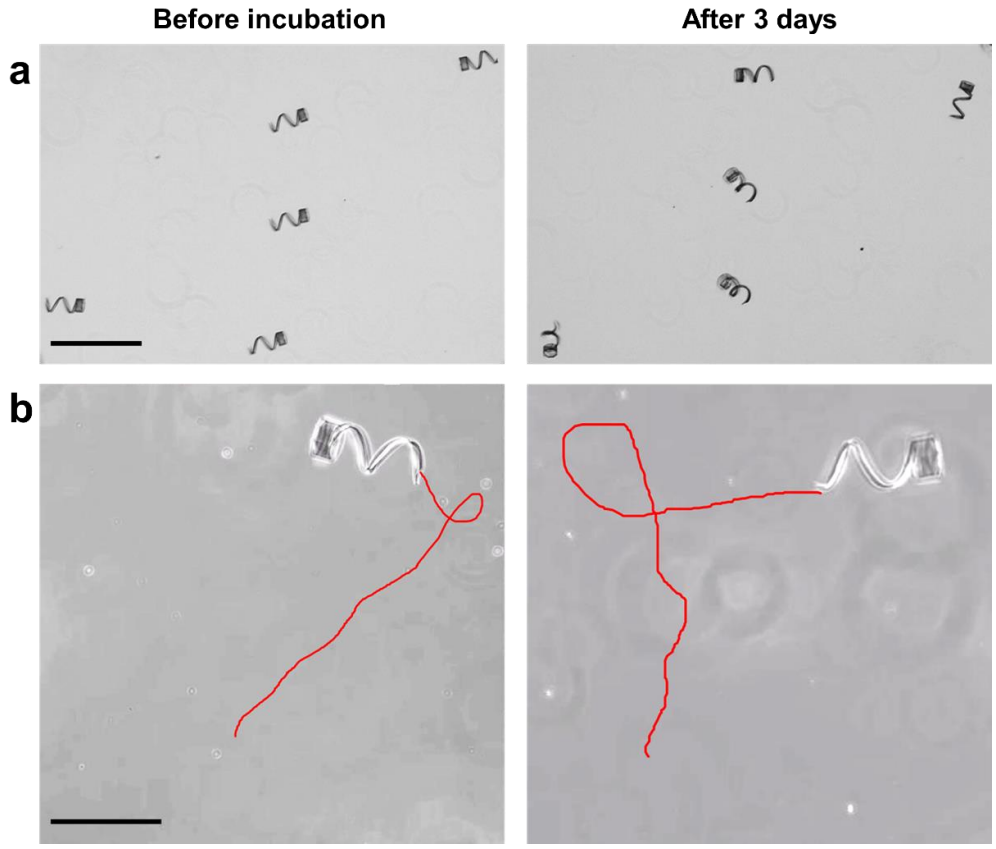

Figure S2. Structural stability test. (a) Microcarrier before and after incubation. Scale bar: 500 µm. (b) Swimming track of microcarriers under magnetic actuation before and after incubation. Trajectory recorded for 4 s. Scale bar: 200 µm. Magnetic field: 10 mT at 65 Hz.

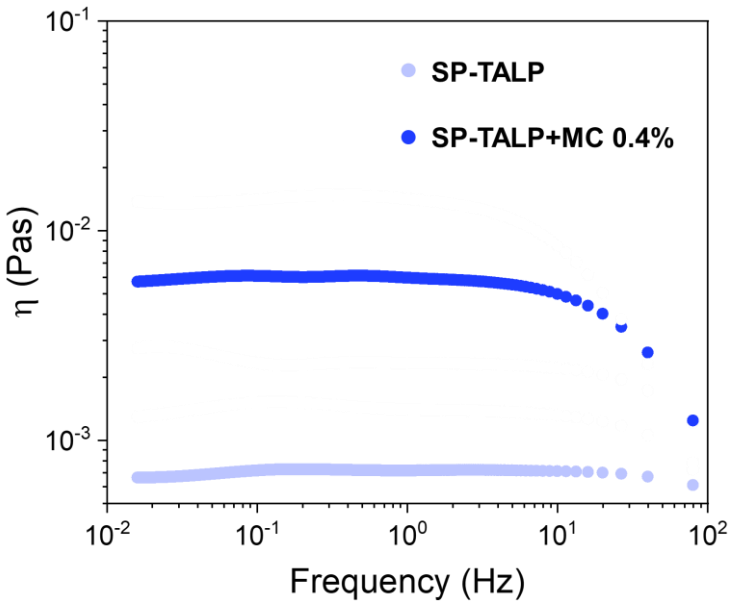

Figure S3. Viscosity measurement of SP-TALP and SP-TALP supplemented with Methylcellulose (MC) 0.4 %. Measurement performed at 38 °C.

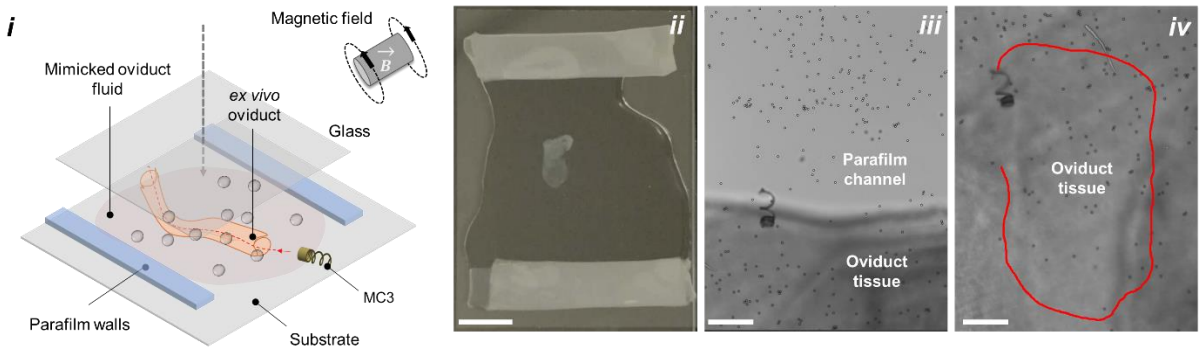

Figure S4. Microcarrier swimming in a mouse oviduct tissue. (i) Schematic. (ii) The oviduct tissue inside a parafilm channel. (iii) Microcarrier entering the oviduct. (iv) Track of a microcarrier swimming in the oviduct. Scale bars: 5 mm for (ii) and 200 µm for the other panels.

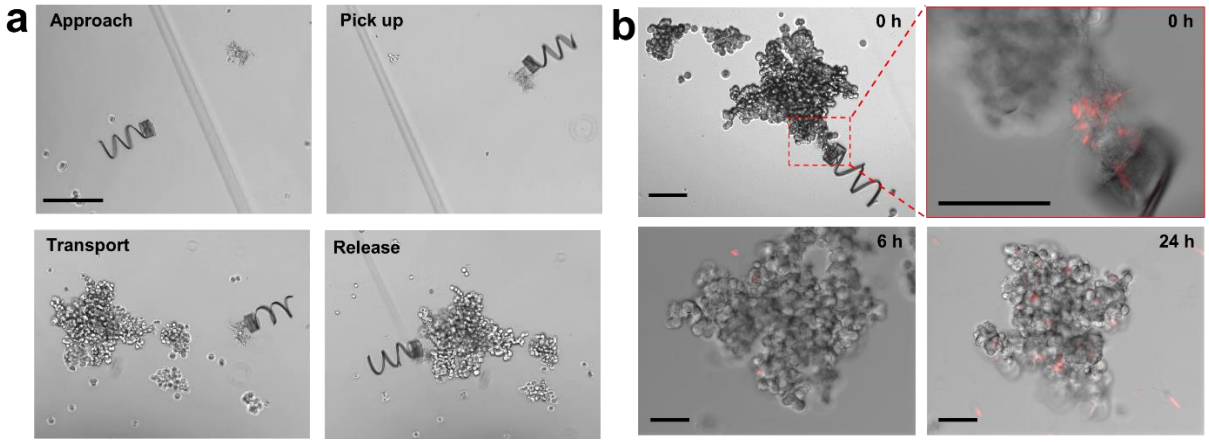

Figure S5. DOX-HCl delivery based on the transport of a sperm immobilized microflake by MC3. (a) Magnetic transport and release of drug-loaded sperm/microflake assembly. Scale bar: 200 μm. (b) DOX-HCl distribution in the cancer spheroid over time. A microflake containing drug-loaded sperm was transported and delivered by MC3. Trypsin was terminated at 20 min after the microflake delivery. Scale bars: 50 μm.

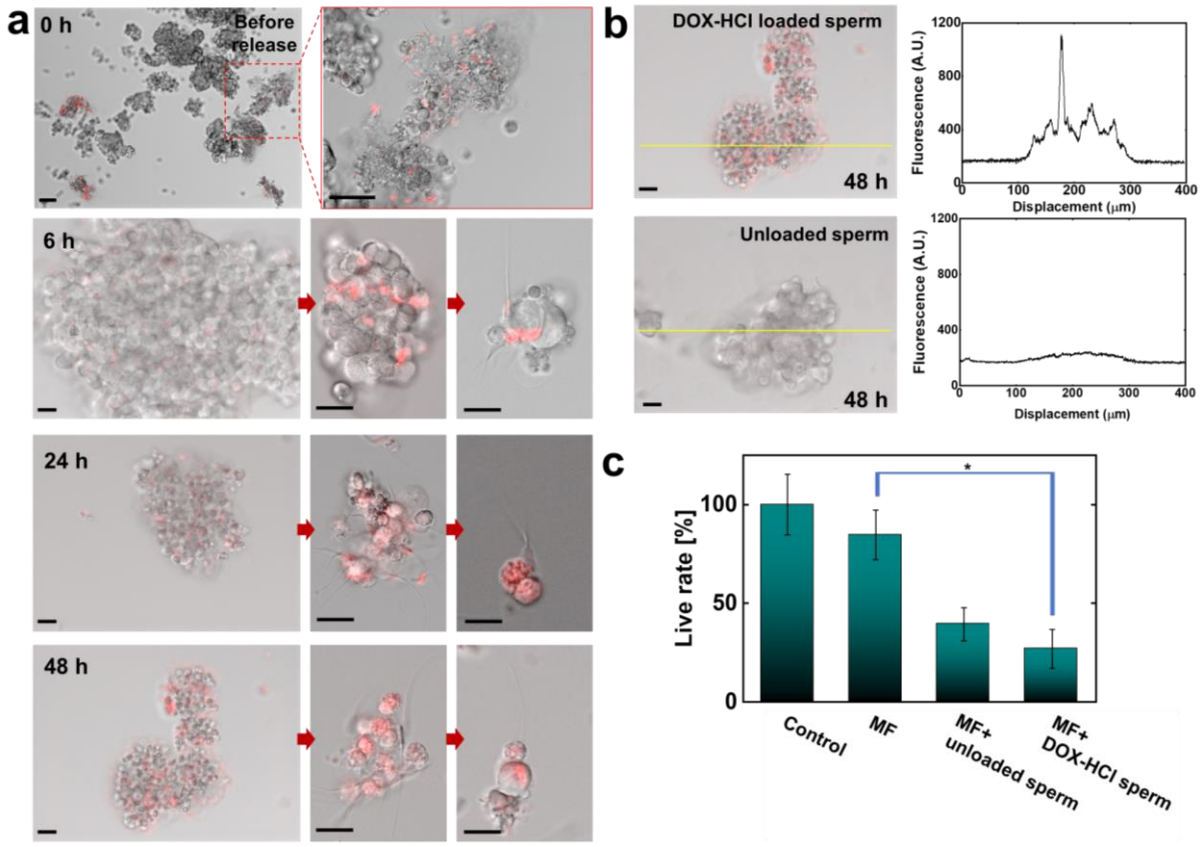

Figure S6. Evaluation of anticancer effect of 10 microflakes immobilized with DOX-HCl loaded sperms (*ca.* 500 DOX-HCl loaded sperms). (a) Fluorescence images showing DOX-HCl distribution in: sperm immobilized microflakes at 0 h before sperm release; targeted HeLa spheroids and clusters over time from 6 h to 48 h after sperm release. Trypsin function

time for sperm release: 20 min. Scale bars: 50 μm and 20 μm in the enlarged image for 0 h; 30 μm for 6 to 48 h. (b) Fluorescence intensity across the spheroids with DOX-HCl loaded sperm as well as unloaded ones. Scale bars: 30 μm. (c) Cell reattachment rate after 48 h of treatment.

Table S1. Single sperm-micromotors reported to date

Type	Fabrication technique of the synthetic part	Coupling mechanism	Key achievements	Year
Tubular spermbot (50 μm long)	Rolled-up	Mechanical	First establishment; Magnetic guidance; Single sperm separation	2013[1]
Tubular spermbot (50 μm long)	Rolled-up	Mechanical	Point-to-point closed-loop motion control	2014[2]
Tubular spermbot (20 μm long)	Rolled-up; Microcontact printing	Mechanical	Improvement on velocity, stability and coupling efficiency	2015[3]
Helical spermbot	Two photon lithography	Mechanical	Immotile sperm transport	2016[4]
Thermoresponsive tubular spermbot	Rolled-up	Mechanical	Thermosensitive release of sperm	2016[5]
Sperm tetrapod	Two photon lithography	Mechanical	Drug loading in sperm; Mechanical release	2018[6]
Sperm-nanoparticles	Chemical synthesis	Endocytosis	Drug loading in sperm; Chemotaxis	2018[7]
Sperm-template microrobot	Chemical synthesis	Electrostatic	Magnetic driving of soft microrobots using sperm as templates	2020[8]

Supporting Information Videos

Video S1. Microcarrier fabrication.

Video S2. Flow simulation of microcarriers.

Video S3. Cargo capture by the microcarriers MC1 and MC3.

Video S4. Flow field around MC3 while rotating in the Z-axis.

Video S5. Microcarrier swimming in a rectangular track under magnetic actuation.

Video S6. Transport of an immotile sperms cluster as a passive cargo model.

Video S7. MC3 swimming in saliva and mimicked oviduct fluid.

Video S8. Microcarriers swimming in 4× diluted bovine blood.

Video S9. MC3 swimming in ex-vivo oviduct channel.

Video S10. Co-incubation of sperms with a microbead.

Video S11. Sperm immobilization onto microflakes.

Video S12. Transport of a sperms-captured microflake by a microcarrier.

Video S13. Enzymatic release of sperms.

Video S14. Microflake hydrolysis at low BSA/HA ratio.

Video S15. Motility of released sperm after microflake hydrolysis.

Video S16. Transport of a microflake immobilized with DOX-HCl loaded sperms toward a HeLa spheroid.